BNL-82075-2009-CP

Point Defect Characterization in CdZnTe

Rubi Gul, Zheng Li, Aleksey Bolotnikov, Kara Keeter,
Rene Rodriquez, and Ralph James

Presented at the IEEE Dresden 2008 Conference
Dresden, Germany
October 19-25, 2008

January 2009

Nonproliferation and National Security Department

Brookhaven National Laboratory
P.O. Box 5000
Upton, NY 11973-5000
www.bnl.gov

Notice: This manuscript has been authored by employees of Brookhaven Science Associates, LLC under Contract No. DE-AC02-98CH10886 with the U.S. Department of Energy. The publisher by accepting the manuscript for publication acknowledges that the United States Government retains a non-exclusive, paid-up, irrevocable, world-wide license to publish or reproduce the published form of this manuscript, or allow others to do so, for United States Government purposes.

This preprint is intended for publication in a journal or proceedings. Since changes may be made before publication, it may not be cited or reproduced without the author's permission.

DISCLAIMER

This report was prepared as an account of work sponsored by an agency of the United States Government. Neither the United States Government nor any agency thereof, nor any of their employees, nor any of their contractors, subcontractors, or their employees, makes any warranty, express or implied, or assumes any legal liability or responsibility for the accuracy, completeness, or any third party's use or the results of such use of any information, apparatus, product, or process disclosed, or represents that its use would not infringe privately owned rights. Reference herein to any specific commercial product, process, or service by trade name, trademark, manufacturer, or otherwise, does not necessarily constitute or imply its endorsement, recommendation, or favoring by the United States Government or any agency thereof or its contractors or subcontractors. The views and opinions of authors expressed herein do not necessarily state or reflect those of the United States Government or any agency thereof.

Printed on recycled paper

Point Defect Characterization in CdZnTe

Rubi Gul, Zheng Li, Aleksey Bolotnikov, Kara Keeter, Rene Rodriguez, Ralph James

***Abstract*–Measurements of the defect levels and performance testing of CdZnTe detectors were performed by means of Current Deep Level Transient Spectroscopy (I-DLTS), Transient Charge Technique (TCT), Current versus Voltage measurements (I-V), and gamma-ray spectroscopy.**

CdZnTe crystals were acquired from different commercial vendors and characterized for their point defects. I-DLTS studies included measurements of defect parameters such as energy levels in the band gap, carrier capture cross sections, and defect densities. The induced current due to laser-generated carriers was measured using TCT. The data were used to determine the transport properties of the detectors under study. A good correlation was found between the point defects in the detectors and their performance.

I. INTRODUCTION

Commercial CdZnTe detectors first appeared on the market in 1990's and subsequently, tremendous effort [1] has been made to increase their efficiency and performance. Efforts [2] have focused on improving the crystal growing techniques with minimal fabrication defects, increasing the effective radiation interaction volume, optimizing the performance, characterizing the materials and devices, and stabilization. Also, the aim is toward more compact readout electronics with less noise and more durability at room temperature.

CdZnTe is a unique material having high density, high band-gap, high resistivity, long electron drift length, low leakage current, and perhaps most importantly high (room temperature) operating temperatures. CdZnTe detectors have high stopping power, low power consumption, low electronic noise, good energy resolution, high detector efficiency, good position sensitivity, and compactness and portability at room temperature. These characteristics of CdZnTe gamma and x-ray detectors are highly desirable in applications such as tomography, x-ray radiology, x-ray CT scan and dental x-ray imaging, imaging [3], space and astronomy, environment, nonproliferation [4], defense and homeland security [5].

To optimize the performance of CdZnTe detectors, it is important to start with material with minimum fabrication or composition-related defects. The purpose of this work was to measure defect parameters of different samples to correlate defect profiles with detector's characteristics and performance. In doing so one may improve the crystal growth and fabrication technology accordingly.

Manuscript received November 14, 2008. This work was supported in part by the U.S. Department of Energy.

R. Gul is with the Brookhaven National Laboratory, Upton NY 11973, USA (telephone: 631-344-7604, e-mail: gul@bnl.gov).
Z. Li is with the Brookhaven National Laboratory, Upton NY 11973, USA
A. Bolotnikov is with the Brookhaven National Laboratory, Upton NY 11973, USA
K. Keeter is with the Idaho State University, Pocatello, ID, 83209, USA
R. Rodriguez, is with the Idaho State University, Pocatello, ID, 83209, USA
R. James is with the Brookhaven National Laboratory, Upton NY 11973, USA

II. EXPERIMENTAL PROCEDURE

We studied two CdZnTe detectors, CZT-2R and CZT-2ev, from two different commercial manufacturers [6,7]. The specifications of these detectors are given in Table I.

TABLE I
SAMPLE SPECIFACTIONS

Sample	Thickness (mm)	Area (mm^2)	ρ x 10^{10} (Ωcm)	τ (μs)	μ (cm^2/sV)	$\mu\tau$ (cm^2/V) x 10^{-3}
CZT-11R	1.1	31	0.4	0.2	570	1.0
CZT-2ev	2.1	102	2.2	3.5	1145	3.9

The study focused on measuring point-defect parameters such as energy levels (E) in the band gap, carrier capture cross sections (σ), and defect densities (N_t) using the I-DLTS technique [8,9]. Induced current caused by laser-generated carriers were measured using TCT [10]. Electrical characteristics were monitored using I-V measurements, and radiation detection performance was tested by gamma-ray spectroscopy using an Am^{241} standard source.

To study the deep levels in the crystals, we employed an I-DLTS system, especially designed for high-resistivity materials, such as CdZnTe and heavily irradiated Si. Two important characteristics of this research are: (1) the technique is applicable for highly resistive materials (>10^6 Ω-cm), and (2) the minimum measurement temperature can be as low as 10 K, which is good for shallow-level measurements. The main components of BNL's I-DLTS system are: a cryogenic cooling system consisting of a He cryostat (10 – 350 K) with temperature controller SI9650; an illumination system for defect filling consisting of a pulse generator HP 8110A that drives lasers with various wavelengths (660 nm to 1030 nm); a Keithley 487 power supply to provide voltage bias to the samples; a Keithley 428 current amplifier to amplify the current transient signal obtained from the charges emitted from filled defect levels; and a Tektronix 7704A oscilloscope to record the current transients. In this research the electron filling of the defect levels is achieved by an 822-nm NIR laser with 4.5-mW optical power at an applied voltage of 10 V, which has an absorption length in CZT comparable to the sample's thickness (~ 2 mm). We note that the illumination system is capable of generating a large number of charge carriers during the trap filling process, resulting in a significantly large transient signal.

In our I-DLTS experiments, the detectors were cooled down to 10 K, and then heated at a constant rate up to about 350 K. The ramp-up temperature step was about 1 K. At each temperature, the defect levels in a sample were first filled at 0 bias voltage by an NIR laser operating at a wavelength of 822 nm with a pulse width of 2 ms and a pulse period of 45 ms. Thus, the defect filling time in a laser pulsing cycle is 2 ms. Then, during the time when the laser was off in a laser pulsing cycle (45 ms - 2 ms = 43 ms), a bias voltage was applied to the sample to efficiently de-trap the charges from previously filled defect levels. The resulting transient current from this de-trapping process was recorded by a fast oscilloscope and read by a PC during the laser-off period in the laser pulsing cycle. The I-DLTS signals were obtained by sampling the differences in the current transient at

two sampling times: t_1 and t_2 at each temperature. The sampling time t_1 was increased in steps from 0.2 ms to 3 ms, while the sampling time t_2 was taken as $4t_1$. Li gives more details of I-DLTS principles and modeling in reference [9]. The energy levels calculated from the I-DLTS signal are those for electron traps, and their energies are measured from the edge of the crystal's conduction band.

The Transient Current Technique (TCT) is used to obtain knowledge about the electrical transport properties of the detectors, such as mobility and electron lifetime. The setup consists of a Keithley 237 power supply, a LeCroy 1-GHz Oscilloscope, and an Agilent 81110A pulse generator. The illumination system contains a 660-nm red laser operated by the Agilent 81110A pulse generator at 10 V during biasing. The width of the pulse is 5 ns, and the period is 10 ms. The described illumination system generates a sufficient number of charge carriers at the surface of the detectors.

III. RESULTS AND DISCUSSIONS

First we measured each detector's photosensitivity by measuring *I-V* curves. A notable shift in the current was observed when detectors were exposed to light, indicating the samples' good photosensitivity. By comparing the leakage current data for the two detectors shown in Fig. 1, it was found that leakage current is 10 times larger for the sample CZT-11R than the second sample CZT-2ev. The resistivity calculated from the *I-V* measurements in the dark for CZT-11R and CZT-2ev, respectively, was 0.4×10^{10} Ω-cm and 2.2×10^{10} Ω-cm.

The spectroscopic responses to gamma radiation of both samples were measured using a standard Am^{241} source. The data were collected at different bias voltages with 500 gain and 2-μs shaping time. Photopeak data were collected at different applied bias voltages. The $\mu\tau_e$ product is determined from the classical Hecht equation. The $\mu\tau_e$ for the first sample, CZT-11R, calculated from the Am^{241} gamma ray spectroscopy is 1.0×10^{-3} cm^2/V and 3.9×10^{-3} cm^2/V for CZT-2ev.

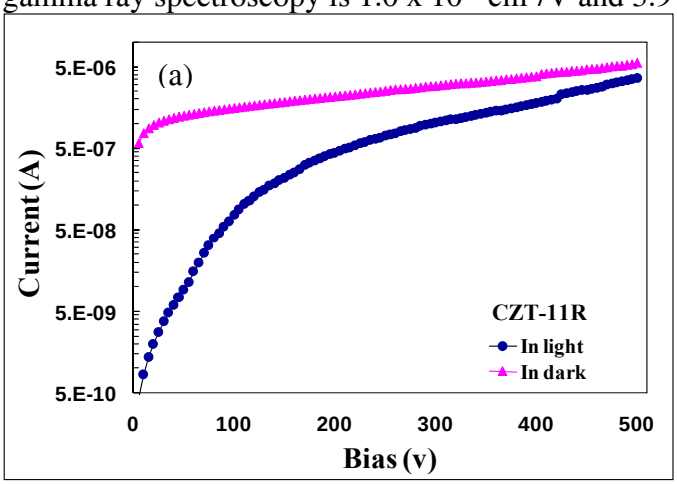

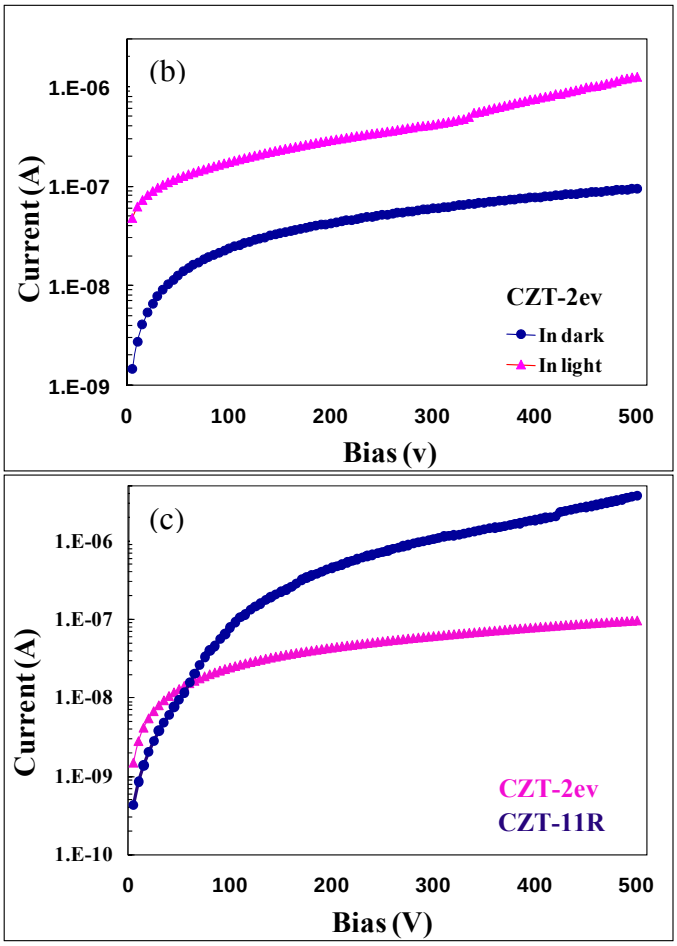

Fig. 1. I-V Characteristic plots; Photo current response of (a) CZT-11R and (b) CZT-2ev; and (c) the leakage current for CZT-11R and CZT-2ev detectors.

TCT results

The transient electron current signal for both detectors was measured by TCT. Charge carriers were generated at the front surface of the detector by illuminating it with a 660-nm laser. The transient electron current signal is induced due to the drift of a sheet of electrons generated within one-micron thickness of the detector's exposed surface. The shapes of the transient electron currents at 1100-V bias are shown in Fig. 3. Both detectors behaved in a similar way. The electron current signal for CZT-2ev is greater than that for the CZT-11R. This indicates the charge collection performance of CZT-2ev is better than CZT-11R. The current decreases with time, indicating a decreasing electric field *E* from the front to the back side of the detector. This may be related to a positive space charge [11]. The flat region near the end of the transient indicates that the electric field at the back is lower than that at the front side of the detector.

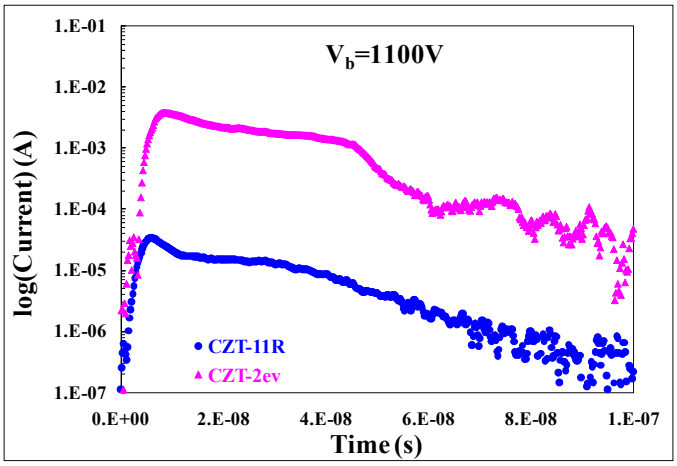

Fig. 2. TCT measurements for CZT-11R and CZT-2ev; Laser-induced transient current signal at 1100-V bias voltage.

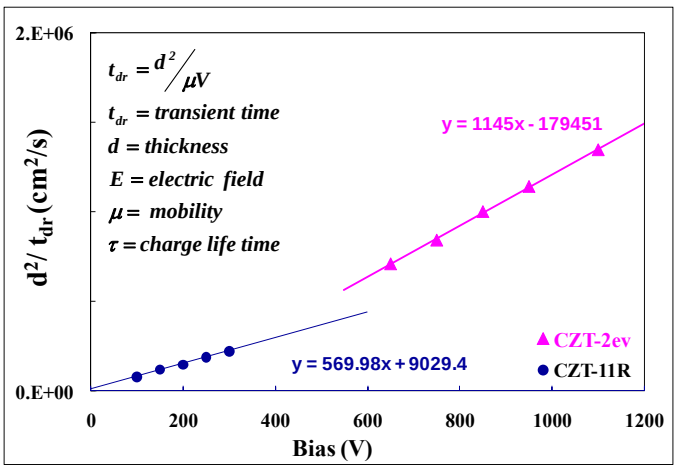

Fig. 3. TCT measurements for CZT-11R and CZT-2ev; Electron mobility measurement which is obtained from the slope of the d^2/t_{dr} Vs. V plot.

The laser induced transient current signal is used to determine the electron mobility in the material. The values for the electron mobility (μ) and carrier life time (τ) are recorded in Table 1 for both detectors under study. The electron mobility and carrier life time values for detector CZT-2ev were found larger than that for detector CZT-11R.

I-DLTS results

The detectors were characterized for energy traps/defects, charge capture cross section of defects and the trap density using I-DLTS. The defects found in these two detectors are point defects, although in detector CZT-2ev there is a broad peak above room temperature which might be the effect of composite defects. I-DLTS signal and Arrhenius plots for the two detectors are shown in Fig. 4 and Fig. 5. The plots in these figures seem very similar, although the energies of the traps are a little different.

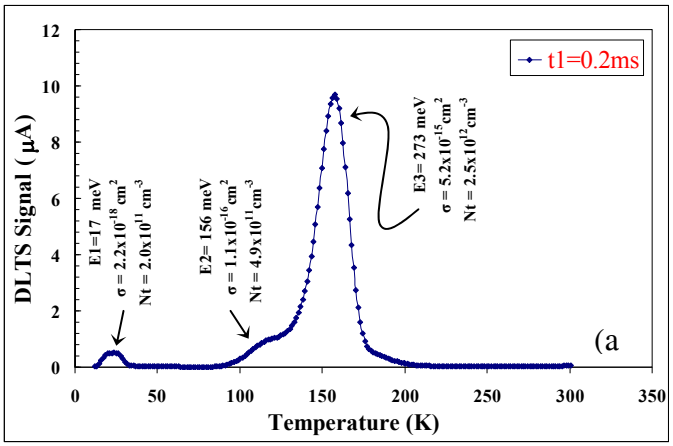

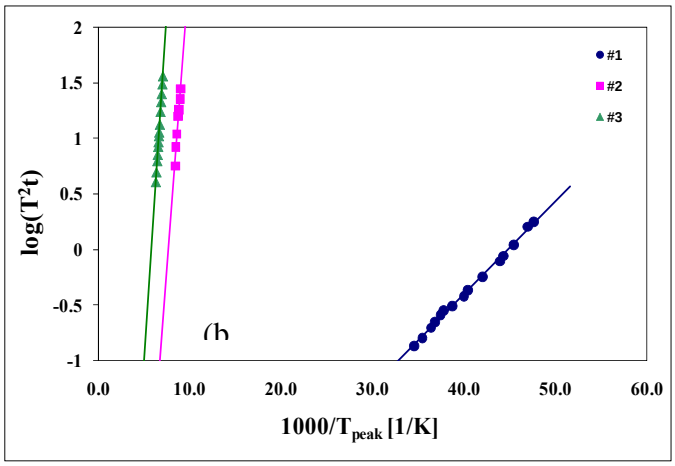

Fig. 4. Defect information for CZT-11R by using I-DLTS; a) Identification of defect levels using a time window t_1=0.2ms. The plot also shows the energy levels, carrier capture cross sections, and the corresponding defect densities; b) Arrhenius plots.

Starting from the lower energy traps at lower temperature, in detector CZT-11R there is one shallow level of (E_c – 17) ± 2 meV± 2 meV in temperature range from 10 K to 30 K. Detector CZT-2ev has one shallow energy trap in this temperature range with comparatively smaller energy trap of about (E_c - 9) ± 2 meV. In addition to this shallow level there is one more level with an energy of (E_c - 52) ± 6 meV in the temperature around 75 K. All these traps in region below 100 K are shallow electron donor traps. There is a big dominant peak in the center of the DLTS plots in both detectors. The energy of this trap is (E_c - 273) ± 24 meV in CZT-11R and (E_c - 228) ± 2 meV in CZT-2ev. In the shoulder of these peaks there is a less dominant trap which has an energy of (E_c - 156) ± 5 meV and (E_c - 158) ± 4 meV. All four traps might be related to the dopant, while in CZT-2ev the shift of the energy level toward the shallow region may be due to the different concentrations of the dopant.

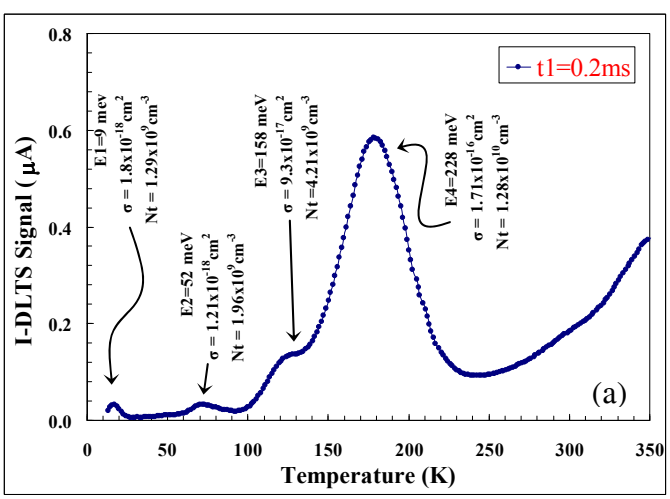

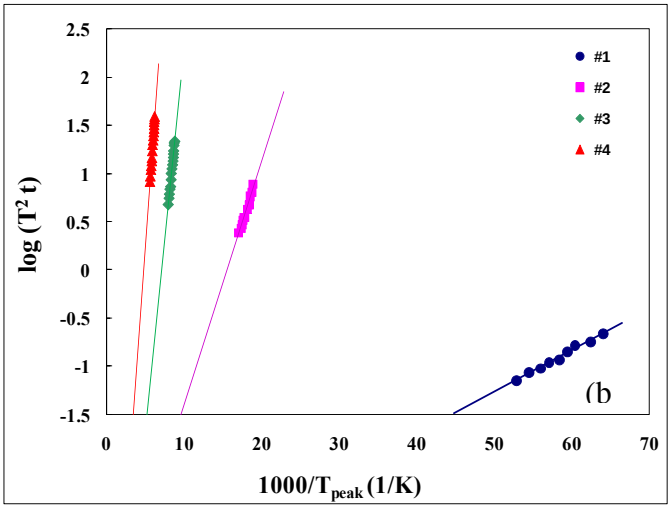

Fig. 5. Defect information for CZT-2ev by using I-DLTS; a) Identification of defect levels using a time window t_1=0.2ms. The plot also shows the energy levels, carrier capture cross sections, and the corresponding defect densities; b) Arrhenius plots.

The carrier capture cross sections of the defect levels seem, in general, to be increasing with the increase of the energy of the trap. The values of capture cross sections for CZT-11R are greater than those for CZT-2ev. The capture cross sections for CZT-11R are from 10^{-18} to 10^{-15} cm^2, while for CZT-2ev it was from 10^{-18} to 10^{-16} cm^2. Comparing the values for each defect level, it appeared that the first three shallow electron traps in both detectors were nearly the same and were as low as 10^{-18} cm^2. Capture cross sections for the next higher shallow levels (~ 157 meV) were in the range of 10^{-16}, which is actually 100 times greater than the previous shallow levels. For the remaining two levels, depending on the energy traps the values were increased by a factor of ~ 10 from the previous levels. The highest energy trap (E_c – 273) + 24 eV in the two detectors had higher capture cross sections, i.e., 5.2 x 10^{-15} cm^2. The charge carrier capture cross-section distribution for both detectors with respect to energy is shown in Fig. 6.

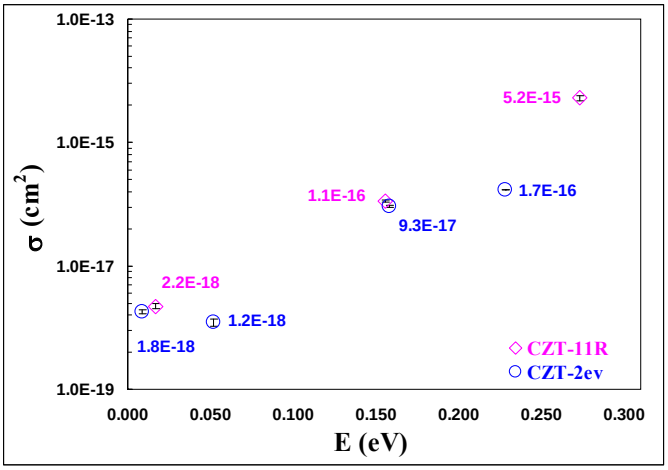

Fig. 6. Carrier capture cross-sections as a function of energy for CZT-11R and CZT-2ev.

The defect densities varied from level to level. If we compare the defect densities results it can be concluded that CZT-11R had ~100 times higher values than CZT-2ev. The values for defects densities for CZT-11R range from 10^{11} to 10^{12} cm^{-3}, while for CZT-2ev the range was from 10^9 to 10^{10} cm^{-3}. The defect densities as function of the energy levels are plotted in Fig. 7. The change in the values of capture cross sections and defect densities are likely related to the controlling environments in the crystal growth process.

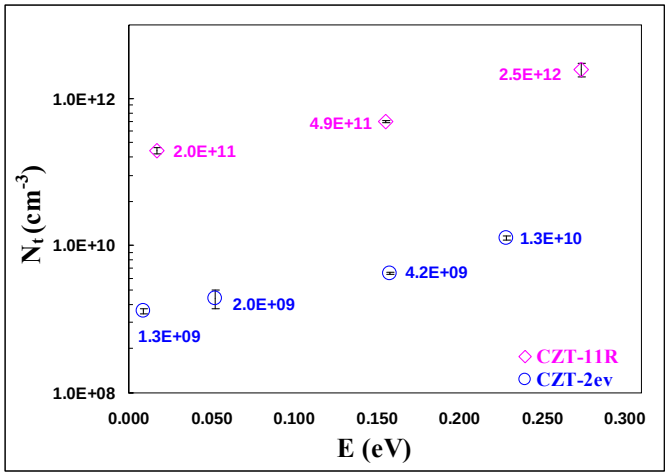

Fig. 7. Defect densities as a function of energy for CZT-11R and CZT-2ev.

Defects related parameters for the energy traps E, charge capture cross-sections σ and defect densities N_t obtained from I-DLTS for both detectors are recorded for each peak in Table II.

TABLE II
SUMMARY OF I-DLTS RESULTS

Sample	Trap #	E (meV)	σ (cm^2)	σ_{error} (cm^2)	N_t (cm^{-3})	N_t St. dev
CZT-R11	1	17±2	2.2×10^{-18}	2.1×10^{-19}	2.0×10^{11}	1.7×10^{10}
	2	156±5	1.1×10^{-16}	4.0×10^{-18}	4.9×10^{11}	$1. \times 10^{10}$
	3	273±24	5.2×10^{-15}	4.5×10^{-16}	2.5×10^{12}	4.9×10^{11}
ZT-2ev	1	9±2	1.8×10^{-18}	1.4×10^{-19}	1.29×10^{9}	1.1×10^{8}
	2	52±6	1.2×10^{-18}	1.5×10^{-19}	1.96×10^{9}	5.8×10^{8}
	3	158±4	9.3×10^{-17}	2.1×10^{-18}	4.21×10^{9}	1.2×10^{8}
	4	228±2	1.7×10^{-16}	1.5×10^{-18}	1.28×10^{10}	7.6×10^{8}

CONCLUSION

Two detectors from different vendors were investigated for the crystal defects and electrical response and radiation response. Both detectors have almost similar point defects except for some difference in trap level and densities. Detector CZT-11R has defect concentrations about 100 times higher than that of CZT-2ev, which correlates nicely with the reduced transport properties (lower mobility and short carrier lifetime), charge collection (less charge collected), electrical properties (higher leakage current), and poor spectroscopy response in CZT-11R as compared to CZT-2ev. A good correlation was found between the higher defect concentrations and the detectors' electrical and radiation response.

References

[1] Parnham, K.B., *Nucl. Instr. and Meth. A,* pp. 487-491, 377 (1996).

[2] Schlesinger, T. E., Toney, J. E., Yoon, H., Lee, E. Y., Brunett, B.A., Franks, L., James, R. A., "Cadmium zinc telluride and its use as a nuclear radiation detector material", *Materials Science and Engineering*, pp. 103-189, 32 (2001).

[3] Giakos, G, C., "A novel collector for imaging detector application", *Proc. IEEE* , pp. 160-163 (1999).

[4] Olsen, R. W., James, R. B., Cofield., Millre, B., Mickelsen, B.,"Special nuclear materials monitoring: An application of CdxZn1-xTe detectors", *Nucl. Instrum. and Meth.in Phys. Res A*, pp. 467-469, 380 (1996).

[5] Hoover, A. S, Baird, B., Kippen, R.M., Rawool-Sullivan, M. W, Sullivan, J.P., "A Compton imaging device for homeland security", *Proc. SPIE* pp. 5540 (2005).

[6] Kimura, H., Komiya, H., *J. Cryst. Growth*, pp. 283-291, 20 (1973).

[7] Doty, F.P., *J. Vac. Sci. Technol. B*, pp. 1418 -1422, 10 (4) (1992).

[8] Li, Z., *Nucl. Instr. and Meth. A*, pp. 399-416, 403 (1998).

[9] Li Z., Li, C.J. , *Materials Science in Semiconductor Processing*, pp.283–287, 9 (2006).

[10] Eremin, V., *Nucl. Instr. and Meth. A,* pp. 388-398, 372 (1996).

[11] Li, Z., *IEEE Trans. Nucl. Sci*., pp. 1901-1908, 55 (2004).